Fermi National Accelerator Laboratory

FERMILAB-Pub-91/164-A
June 1991

Aspects of Reheating in First-Order Inflation

Richard Watkins

Department of Astronomy and Astrophysics
Enrico Fermi Institute
The University of Chicago
Chicago, IL 60637 U.S.A.

NASA/Fermilab Astrophysics Center
Fermi National Accelerator Laboratory
P.O. Box 500, Batavia, IL 60510 U.S.A.

Lawrence M. Widrow

Canadian Institute for Theoretical Astrophysics
University of Toronto
60 St. George Street
Toronto, ON M5S 1A1 Canada

Abstract

We study reheating in theories where inflation is completed by a first-order phase transition. In these scenarios, the Universe decays from its false vacuum state by bubble nucleation. In the first stage of reheating, vacuum energy is converted into kinetic energy for the bubble walls. To help understand this phase we derive a simple expression for the equation of state of a universe filled with expanding bubbles. Eventually, the bubble walls collide. We present numerical simulations of two-bubble collisions clarifying and extending previous work by Hawking, Moss, and Stewart. Our results indicate that wall energy is efficiently converted into coherent scalar waves. We go on to discuss particle production due to quantum effects. These effects lead to the decay of the coherent scalar waves. In addition, they lead to direct particle production during bubble-wall collisions. We calculate particle production for colliding walls in both sine-Gordon and ϕ^4 theories and show that it is far more efficient in the ϕ^4 case. The relevance of our work for recently proposed models of first-order inflation is discussed.

1. Introduction

In Guth's original version of inflation [1], the Universe decays from its initial false-vacuum state by the nucleation of true-vacuum bubbles. As the bubbles expand, the energy in the false vacuum is converted into kinetic energy for the bubble walls. In theory, the walls eventually collide, the true vacuum percolates, and wall energy is converted into radiation, reheating the Universe. Unfortunately, in Guth's model the nucleation and expansion of bubbles cannot keep up with the exponential expansion of the regions still trapped in the false vacuum, and the true vacuum never percolates [2]. This is known in the literature as the 'graceful exit' problem.

Clearly, first-order inflation (generically, any model in which inflation is completed by a strongly first-order phase transition) can work if either the nucleation or expansion rate changes during the inflationary phase. For example, in the extended inflation scenario proposed by La and Steinhardt [3] the Hubble parameter in the vacuum-energy dominated ($p = -\rho$) Universe decreases with time, thus enabling the true vacuum to percolate. While La and Steinhardt's proposal suffered a graceful exit problem of its own [4], there has been no shortage of theories which purport to save the general idea of first-order inflation [5].

Given the renewed interest in first-order inflation, we felt it an opportune time to examine some of the nuts and bolts of reheating in these models. Reheating in new [6] and chaotic [7] inflation has been examined in some detail [8]. The analysis in these scenarios is simplified by the fact that the Universe can be treated as homogeneous (Friedmann-Robertson-Walker) throughout. Inflation occurs when some order parameter or scalar field finds itself displaced from the minimum of its potential. At first, the field slowly rolls towards this minimum. During this phase the energy density ρ of the Universe is dominated by vacuum energy with $\rho = \text{const}' \equiv \rho_{vac}$; the pressure $p = -\rho$; and the scale factor $a \propto e^{H_I t}$, where $H_I^2 = 8\pi\rho_{vac}/3m_{pl}^2$. (We use units where $\hbar = c = k_B = 1$ and $m_{pl} = G_{\text{Newton}}^{-1/2} \simeq 10^{19}\text{GeV}$ is the Planck mass). As the inflaton reaches the minimum, the slope of the potential increases and the field begins to oscillate about the minimum on a time scale short compared to the Hubble time. These oscillations behave at first like pressureless nonrelativistic matter so that $a \propto t^{2/3}$. Eventually, the oscillations decay into relativistic particles and the Universe becomes radiation-dominated. We note that if the lifetime of the inflaton is long compared to H_I^{-1}, most of the energy in the ϕ field will be diluted by cosmological expansion and the reheat temperature T_{RH} ($\sim (m_{pl}\Gamma_\phi)^{1/2}$) will be well below $\rho_{vac}^{1/4}$, the energy scale associated with the false vacuum.

The physics of reheating in first-order inflation is essentially the same as in new and chaotic inflation: Energy initially stored in a coherent scalar field must be converted into radiation. However, the situation is considerably more difficult to analyze. Here, both the field ϕ and the metric are inhomogeneous. Furthermore, reheating involves a mix of quantum physics (bubble nucleation and particle creation) and classical physics (expansion and collisions of bubbles). Difficulties aside, a number of authors have focused on the potentially rich phenomenology associated with these scenarios. For example, it has been suggested that gravitational waves [9], black holes [10][11], topological defects [12], and the baryon asymmetry [13][11] may have been produced during the phase transition. Whether or not such phenomena actually occur depends in part on the details of reheating. For though any asymmetric double-well potential will do. We shall generically refer to models of this type as ϕ^4 models. Focus for the moment on the case where $\epsilon \ll \lambda$ so that the energy difference between true and false minima is small compared to the height of the barrier. To lowest order in ϵ, the true and false minima are at $-\phi_o$ and ϕ_o respectively. The mass of ϕ-excitations in either of these minima is given by $m_\phi = \lambda^{1/2}\phi_o$, and $\rho_{vac} = 2\epsilon\phi_o^4$. $\epsilon \ll \lambda$ corresponds to the thin-wall limit in which the radius of the bubbles is much greater than the thickness of the wall separating the interior true vacuum region from the exterior false vacuum region. One nice feature of the thin-wall limit is that the properties of individual bubbles can be determined analytically. In particular, the thickness of the bubble wall is $\Delta = 2/\left(\lambda^{1/2}\phi_o\right) = 2m_\phi^{-1}$, the surface energy density is $\sigma = 2\lambda^{1/2}\phi_o^3/3$, and the radius of the bubble at the time of nucleation is $R_o = \lambda^{1/2}/\left(\epsilon\phi_o\right) = 3\sigma/\rho_{vac}$. $R_o/\Delta \simeq \lambda/\epsilon \gg 1$ so the bubble walls are indeed thin.

The results quoted above are valid so long as gravity is not important. Gravity becomes important when the radius of the bubbles becomes comparable to the Hubble radius [16]. For the case at hand, the Hubble radius is given by $H^{-1} = \left[8\pi\rho_{vac}/3m_{pl}^2\right]^{-1/2} \simeq m_{pl}/\left(\epsilon^{1/2}\phi_o^2\right)$. $RH \simeq (\lambda/\epsilon)^{1/2}\,\phi_o/m_{pl}$ is therefore a measure of how important gravity is.

The nucleation rate per unit volume (number of bubbles nucleated per unit four-volume) is [17]

$$\Gamma \simeq A\,(m_\phi)^4\,e^{-S_E} \tag{2.3}$$

where A is a constant of order unity and S_E is the Euclidean action for the bounce solution corresponding to a critical bubble. For the thin wall case, $S_E = \pi^2\lambda^2/3\epsilon^3$. Perhaps the most important parameter describing a first-order inflation theory is $\eta \equiv \Gamma/H^4$, the so-called percolation parameter. η gives roughly the number of bubbles nucleated per horizon volume per Hubble time. For the case at hand

$$\eta \simeq \left(\frac{\lambda}{\epsilon}\right)^2\left(\frac{m_{pl}}{\phi_o}\right)^4\, e^{-\pi^2\lambda^2/3\epsilon^3}\ . \tag{2.4}$$

The requirement that inflation last long enough to solve the horizon and flatness problems constrains η to be less than about 10^{-3}, whereas percolation of the true vacuum bubbles can only occur if $\eta > O(0.1)$. In Guth's model, η is constant and the model is untenable. In the models of Ref.[5] , η varies in time; a period of inflation with $\eta < 10^{-3}$ precedes the percolation phase in which η is large.

The mean separation between bubbles is roughly $D \simeq \Gamma^{-1/4} = \eta^{-1/4}H^{-1} \simeq \left(\lambda^{1/2}\phi_o\right)^{-1} e^{S_E/4}$. Certainly, a key unknown is the value (or range of values) η has when percolation occurs. (Remember that η is increasing with time.) For $\eta \gg 1$, D will be less than the Hubble radius and there will be many bubbles within a given Hubble volume. In this case, cosmological expansion can be neglected in treating the dynamics of the bubbles. On the other hand, if $\eta \sim 1$ when percolation occurs, D will be of order the horizon and cosmological expansion will play an essential role in the bubble dynamics. In what follows we will neglect, for the most part, cosmological expansion in treating the bubbles, but only because it simplifies the calculations. We leave the full problem of bubble dynamics in an expanding spacetime for future investigations.

Let T^W_{ab} be the stress energy for the wall. In the thin wall approximation T^W_{ab} has a δ-function singularity across the wall. It is convenient to define the quantity

$$S_{ab} \equiv \int dl\, T^W_{ab} \tag{3.3}$$

where l is the proper distance through the surface in the direction of ξ_a. We note that $dl = \gamma dr$.

The three metric intrinsic to the wall is

$$h_{ab} = g_{ab} - \xi_a \xi_b \;. \tag{3.4}$$

For domain walls, $S_{ab} = -\sigma h_{ab}$. In addition bubbles nucleated by quantum tunneling have $3\sigma/R_o = \rho_{vac}$. It is straightfoward to show that

$$\begin{aligned} \Omega^{-1} \int d^3x T^W_{00} &= \frac{3\gamma\sigma R^2}{D^3} \\ &= \rho_{vac} \frac{R^3}{D^3} \\ \Omega^{-1} \int d^3x T^W_{ii} &= \rho_{vac} \frac{R^3}{D^3} \left(\frac{1}{\gamma^2} - \frac{1}{3} \right) \;. \end{aligned} \tag{3.5}$$

Combining Eq.(3.2) and Eq.(3.5) we find

$$\begin{aligned} \bar{\rho} &= \rho_{vac} \\ \bar{p} &= -\rho_{vac} \left(1 + \left(\frac{R}{D} \right)^3 \left(\frac{4}{3} - \frac{1}{\gamma^2} \right) \right) \;. \end{aligned} \tag{3.6}$$

For $R \ll D$, $\bar{p} \simeq -\rho_{vac}$ as expected; the Universe in this case is essentially dominated by vacuum energy. If, on the other hand, bubbles are nucleated with $R_o \simeq D$, then $\bar{p} = -2\bar{\rho}/3$ right after nucleation. This is just the equation of state for a wall-dominated Universe. In fact, the Universe is still undergoing power-law inflation when the bubbles first collide [20]. Finally, if $R_o \ll D$, the walls will be relativistic by the time they collide, and the equation of state just before bubble collisions will be $\bar{p} = \bar{\rho}/3$.

4. Bubble Collisions: Classical Treatment

Bubble collisions provide the next step in reheating. Collisions release energy bound in the walls through both quantum and classical processes. Quantum effects will be discussed in Section 5. Here, we treat the bubble walls as classical field configurations and show that classical scalar waves are emitted during a collision. We explore this process by studying the collision of two expanding bubbles.

For $|r| < |t|$ (Region II), we require a different coordinate system $(\rho', \psi', \theta, \varphi)$ with

$$
\begin{aligned}
x &= \rho' \sinh\psi' \sin\theta \cos\varphi \qquad & z &= \rho' \sinh\psi' \cos\theta \\
y &= \rho' \sinh\psi' \sin\theta \sin\varphi \qquad & t &= \rho' \cosh\psi' \ .
\end{aligned}
\tag{4.2}
$$

In order to find the field configuration in this region one needs to take the field configuration on the $\rho = 0$ hypersurface (from the Region I solution) and evolve into Region II. Since the field configuration only depends on ρ this amounts to solving an ordinary differential equation. For a single thin-wall bubble, the bubble wall is entirely in Region I. The field is essentially constant in Region II, so that evolving the field is usually unnecessary.

The situation changes with more than one bubble. Consider the nucleation of two bubbles. In general this is a complicated process and one that has yet to be treated in the literature. If, however, the bubbles are widely separated at the time of nucleation, then they can be treated as noninteracting (the dilute instanton approximation), and the generalization from the single bounce solution is straightfoward. For two bubbles, the axis joining their centers will be a preferred direction, so that the solution to the Euclidean equations of motion for noninteracting bubbles will have $O(3)$ symmetry. We consider first a coordinate system in which the $\tau = 0$ hypersurface intersects the centers of the two bubbles. The field configuration on this hypersurface becomes initial data for two simultaneously nucleated expanding bubbles in Minkowski space, and one could solve for the field configurations numerically by solving the classical equations of motion. As in the single bubble case, a more efficient technique for finding the evolution exploits the extra boost symmetry of the problem. Here the $O(3)$ symmetry of the two-bubble Euclidean bounce translates to an $O(2,1)$ symmetry in Minkowski space. Let the z-axis correspond to the the line connecting the centers of the bubbles. As before, spacetime is divided into two regions. For $|t| < \sqrt{x^2 + y^2}$ we choose the coordinates (s, ψ, θ, z) with

$$
\begin{aligned}
x &= s \cosh\psi \sin\theta \qquad & z &= z \\
y &= s \cosh\psi \cos\theta \qquad & t &= s \sinh\psi \ .
\end{aligned}
\tag{4.3}
$$

The solution in this region of spacetime is given by the analytic continuation of the two bubble bounce solution. For $|t| > \sqrt{x^2 + y^2}$ we take

$$
\begin{aligned}
x &= s' \sinh\psi' \sin\theta \qquad & z &= z \\
y &= s' \sinh\psi' \cos\theta \qquad & t &= s' \cosh\psi' \ .
\end{aligned}
\tag{4.4}
$$

To find the field configuration in this region, we take the solution on the $t = r \equiv \sqrt{x^2 + y^2}$ hypersurface and solve the equations of motion. Here the equations we are required to solve are $1 + 1$ (s and z) partial differential equations. For the two bubble case, all of the interaction between the bubbles takes place in this second region.

The procedure outlined above was developed and used by HMS. Here we consider bubbles in a theory described by Eqs.(2.1,2.2) with $\epsilon = 0.1$. In Fig. 1a, we show the field $\phi(s, z)$ in the collision region for two simultaneously nucleated bubbles. In Fig. 1b, the an observer at $z = 0$ but arbitrary r, $\tau(r) = \sqrt{t_f^2 + r^2} - \sqrt{t_i^2 + r^2}$. For $r \ll (t_i, t_f)$, $\tau(r) = \tau_0 \left(1 - r^2/2t_i t_f\right)$ whereas for $r \gg (t_i, t_f)$, $\tau(r) = \tau_0 \left(t_i + t_f\right)/2r$. In either case, the time interval decreases with increasing r, a result which can be read off of Fig. 2.

We have carried out a variety of numerical studies and found that generally the radiation of scalar waves is reasonably efficient. For example, in the simulations described above we find that most of the energy in the center of the two-bubble system is radiated away after only a few collisions. This result holds for a wide range of initial separations. We have also simulated the collision of two infinite plane walls in a theory with a symmetric double well potential (Eq.(2.2) with $\epsilon = 0$) and find that the percentage of energy radiated during a single collision is roughly constant and $\sim 30-40\%$ for a wide range ($0.3 < \gamma < 10$) of initial velocities (see, for example, Ref.[21]).

One can also consider first-order inflation in sine-Gordon (SG)-type theories. Here the potential is of the form

$$V = \lambda\phi_o^4 \left(\cos\left(\frac{\pi N \phi}{\phi_o}\right) + V_A(\phi)\right) \tag{4.5}$$

where there are N local minima at $\phi = 2n\phi_o$ and V_A creates a small asymmetry among these minima. For the most part, the dynamics of wall-wall interactions is determined by the first term in V. As is well known, SG kinks in a theory with $V_A = 0$ are true solitons, and infinite plane-symmetric walls pass through one another without dissipating any energy. However, if the walls are curved (or if $V_A \neq 0$) they will produce scalar radiation [22], though not as efficiently as ϕ^4 walls. Reheating, in fact may be very different in these models (see also Section 5), though no detailed work has yet been done.

5. Particle Production

In order to reheat the Universe, the inflaton must couple to ordinary particles. This will allow the classical scalar waves described above to decay, eventually filling the Universe with a thermal bath at a temperature T_{RH}. These couplings also lead to direct production of particles during collisions between walls.

In this section we discuss this direct particle production. In particular, we consider production of fermions arising from interactions of the form $\mathcal{L}_1 = g_1\phi\bar{\psi}\psi$ and $\mathcal{L}_2 = g_2 f^{-1}\bar{\psi}\gamma_\mu\psi\partial^\mu\phi$, where f has units of mass. $\mathcal{L}_1$ is the typical Yukawa coupling of a scalar field to fermions. $\mathcal{L}_2$-type couplings arise if ϕ is a Goldstone (or pseudo-Goldstone) boson. In this case, the potential for ϕ is of the sine-Gordon (SG) type. As we will see, particle production in these two theories is dramatically different, though this is due as much to the peculiar properties of the SG walls as to the different form of the coupling between ϕ and ψ.

Our philosophy is to treat ϕ (the bubbles or walls) as a classical, external field and the fermions as quantum fields in the presence of this source (see, for example, Ref. [23]). In so doing we make no attempt to treat backreaction of particle production on the evolution of the walls.

As a first example, consider an infinite plane-symmetric domain wall. To keep things simple we assume a model with degenerate vacua so that a noninteracting wall will move with constant velocity. Since the result must be Lorentz-invariant, we can work in the rest frame of the wall. Clearly, in this frame $p_0 = 0$ for all modes, so that $p^2 < 0$ and there is no particle production.

Next, consider the head-on collision of two plane-symmetric walls. The walls can come from either ϕ^4 or SG theories. As we will see, the crucial difference between the two models is that ϕ^4 walls scatter off one another while SG walls pass through one another.

In principle, the calculation should be straightforward. One starts with the field configuration describing a collision. In the case of plane-symmetric walls moving in the z-direction, $\phi(\vec{x}, t) = \phi(z, t)$. The next step is to calculate the Fourier transform. Here $\tilde{\phi}(\vec{k}, \omega) = (2\pi)^2 \delta(k_x)\delta(k_y)\tilde{\phi}(k_z, \omega)$. The final step is to substitute into Eq.(5.7) and integrate over p. This will give the number of particles produced per unit area:

$$\frac{N}{A} = 2 \int \frac{dk\, d\omega}{(2\pi)^2} |\tilde{\phi}(k, \omega)|^2 \, \mathrm{Im} \left(\tilde{\Gamma}^{(2)} \left(\omega^2 - k^2 \right) \right) \tag{5.8}$$

where $k \equiv k_z$.

The field configuration for colliding ϕ^4-walls can be found numerically. However, the result will be quite complicated, as the scattering of two ϕ^4 walls is inelastic. In general, scalar waves are produced in the collision whose decay will contribute to the particle production. It is difficult to untangle this contribution from that of the actual collision. We therefore choose to model the collision by treating the walls as infinitesimally thin and assuming that the scattering is perfectly elastic. This model should give accurate results for $k \ll \gamma m_\phi$ and $\omega \ll \gamma m_\phi / v$ in the case of relativistic walls.

Our ansatz for the field configuration is

$$\phi = \begin{cases} \phi_0, & \text{for } vt < z < -vt \text{ and } t < 0; \\ \phi_0, & \text{for } -vt < z < vt \text{ and } t > 0; \\ -\phi_0, & \text{otherwise} \end{cases} \tag{5.9}$$

and the Fourier transform of the field is

$$\tilde{\phi}(\vec{k}, \omega) = \frac{8v\phi_0}{\omega^2 - k^2 v^2} \,. \tag{5.10}$$

The slow power law-fall off at large $\omega^2 - k^2 v^2$ is due to the fact that in our ansatz, ϕ is discontinuous. For realistic "thick" domain walls, $\tilde{\phi}$ would cut off exponentially for $k \gtrsim \gamma m_\phi$ and $\omega \gtrsim \gamma m_\phi / v$. Substituting Eqs.(5.5,5.10) into Eq.(5.7) we estimate

$$\frac{N}{A} \simeq g_1^2 \phi_o^2 \ln \left(\frac{\gamma m_\phi}{2\mu} \right) \tag{5.11}$$

where we have assumed that $\gamma m_\phi \gg 2\mu$ and $\gamma \gg 1$. The energy per unit area radiated by the walls is

$$\frac{E}{A} \simeq g_1^2 \phi_o^2 \gamma m_\phi \tag{5.12}$$

The final result can be written in the form

$$\tilde{\phi}(\omega, k) \simeq \frac{4\pi\phi_o}{\gamma^4 m_\phi^2} \frac{\sinh\left(\frac{\pi\omega}{2\gamma v m_\phi}\right)}{\cosh\left(\frac{\pi\omega}{\gamma v m_\phi}\right) - \cosh\left(\frac{\pi k}{\gamma m_\phi}\right)} . \tag{5.20}$$

This result is similar in many respects to Eq.(5.10). For $\omega < \gamma v m_\phi$ and $k < \gamma m_\phi$, $\tilde{\phi} \propto \left(\omega^2 - v^2 k^2\right)^{-1}$. In addition $\tilde{\phi}$ is exponentially damped for larger values of k and ω, as anticipated above. We estimate that the number of particles produced per unit area is

$$\frac{N}{A} \simeq g_2^2 \phi_o^2 \left(\frac{m_\phi}{\gamma f}\right)^2 \tag{5.21}$$

and the energy lost per unit area is

$$\frac{E}{A} \simeq g_2^2 \phi_o^2 \gamma m_\phi \left(\frac{m_\phi}{\gamma f}\right)^2 \tag{5.22}$$

where again we have assumed that $\gamma m_\phi \gg 2\mu$. This represents a fraction $(g_2 m_\phi/\gamma f)^2$ of the total energy in the walls and is less than that found in the ϕ^4 case by a factor $(m_\phi/f)^2\gamma^{-2}$. The $(m_\phi/f)^2$ term comes from the nature of the coupling $\mathcal{L}_2$ and is usually quite small.

Particle production in this case is due to a slight slowing down of the walls during their interaction. As γ becomes large, the forces between the walls are able to effect a smaller change in velocity, leading to a smaller result for N/A. In principle, there will be similar effects in the ϕ^4 case leading to corrections of order $1/\gamma^n$ to Eqs. (5.11) and (5.12).

Evidently, we can produce particles up to energy γm. If the bubble walls are highly relativistic when they collide, there will be the possibility of producing particles well above the mass of the inflaton.

6. Conclusions

It is relatively easy to find a cosmological scenario which inflates. The challenge is in bringing an end to inflation so that the resultant universe resembles the one we live in. The vacuum energy which drives inflation must be converted into relativistic particles. Furthermore, fluctuations which arise during inflation should not lead to unacceptably large distortions in the microwave background. It is a bonus if they provide the seed perturbations necessary to drive the formation of large-scale structure. In addition, relics of the inflationary epoch such as gravity waves and topological defects may have survived until the present epoch. If detected these phenomena would provide a window to the very early Unverse.

The search for a truly graceful exit from inflation has had limited success. As is well known, most new and chaotic inflation scenarios require 'fine tuning' to satisfy the black, the true vacuum in light gray. Regions where $\phi < -\phi_o$ appear white. In Fig. 1b the initial separation beteen the bubbles has been doubled and the coordinates have been scaled by a factor 1/2.

2. Spacetime diagram in the $t - r$ plane for the two-bubble collision shown in Fig. 1a. For this diagram, $z = 0$.
3. Field configuration shown at different times during the collision. Note the scalar radiation emanating from the collision region.
4. Spacetime diagrams illustrating a big bubble hitting a small bubble. Fig. 4a shows the two-bubble collision in the equal bubble (simultaneous-nucleation) frame. Here, the radiation is symmetric about $z = 0$. Fig. 4b shows the same configuration in a Lorentz-boosted frame. The bubble on the left is nucleated first and is larger at the time of the collision. In this frame, all of the radiation is moving to the right, away from the nucleation site of the big bubble.

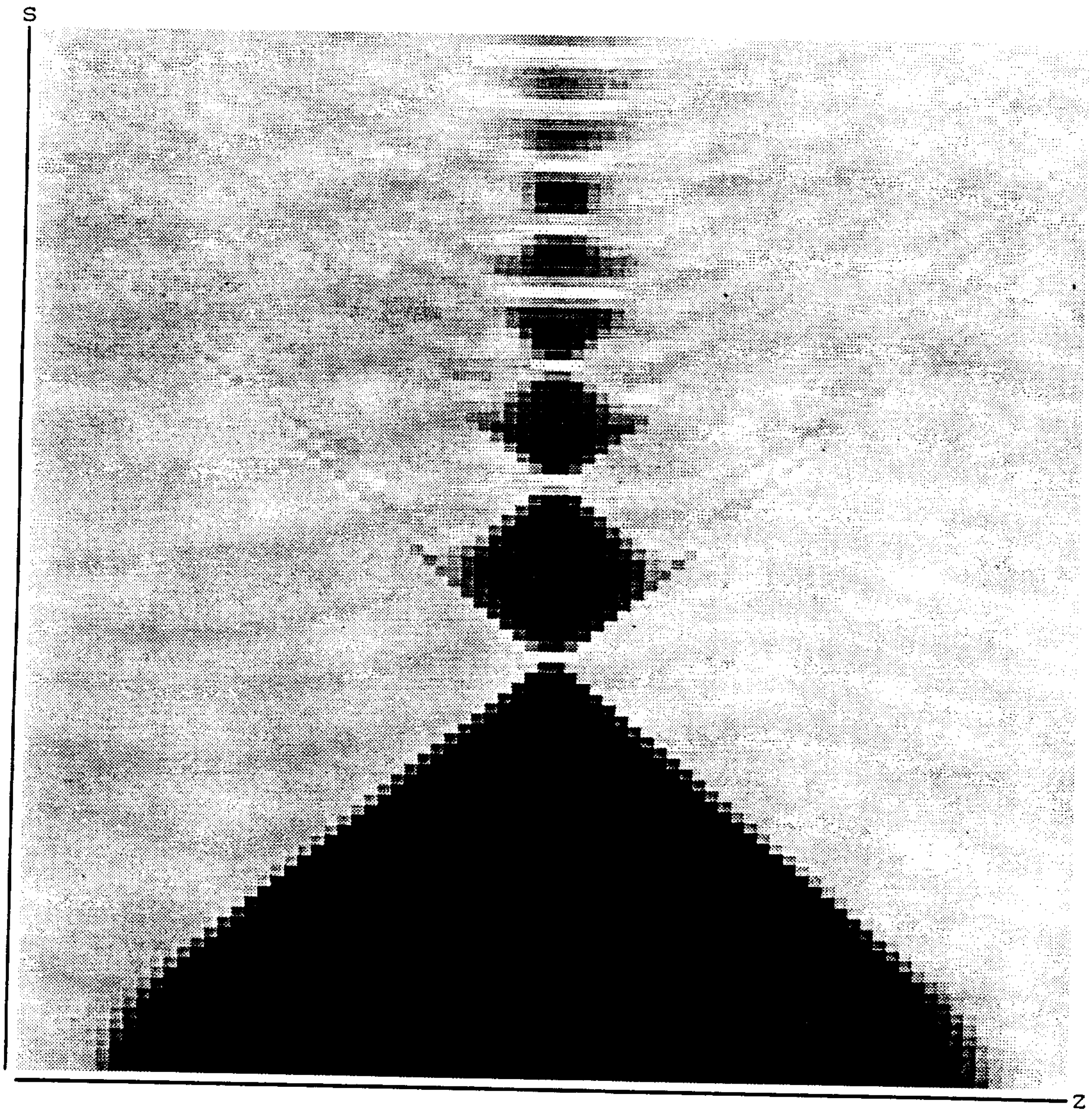

- FIG 1a -

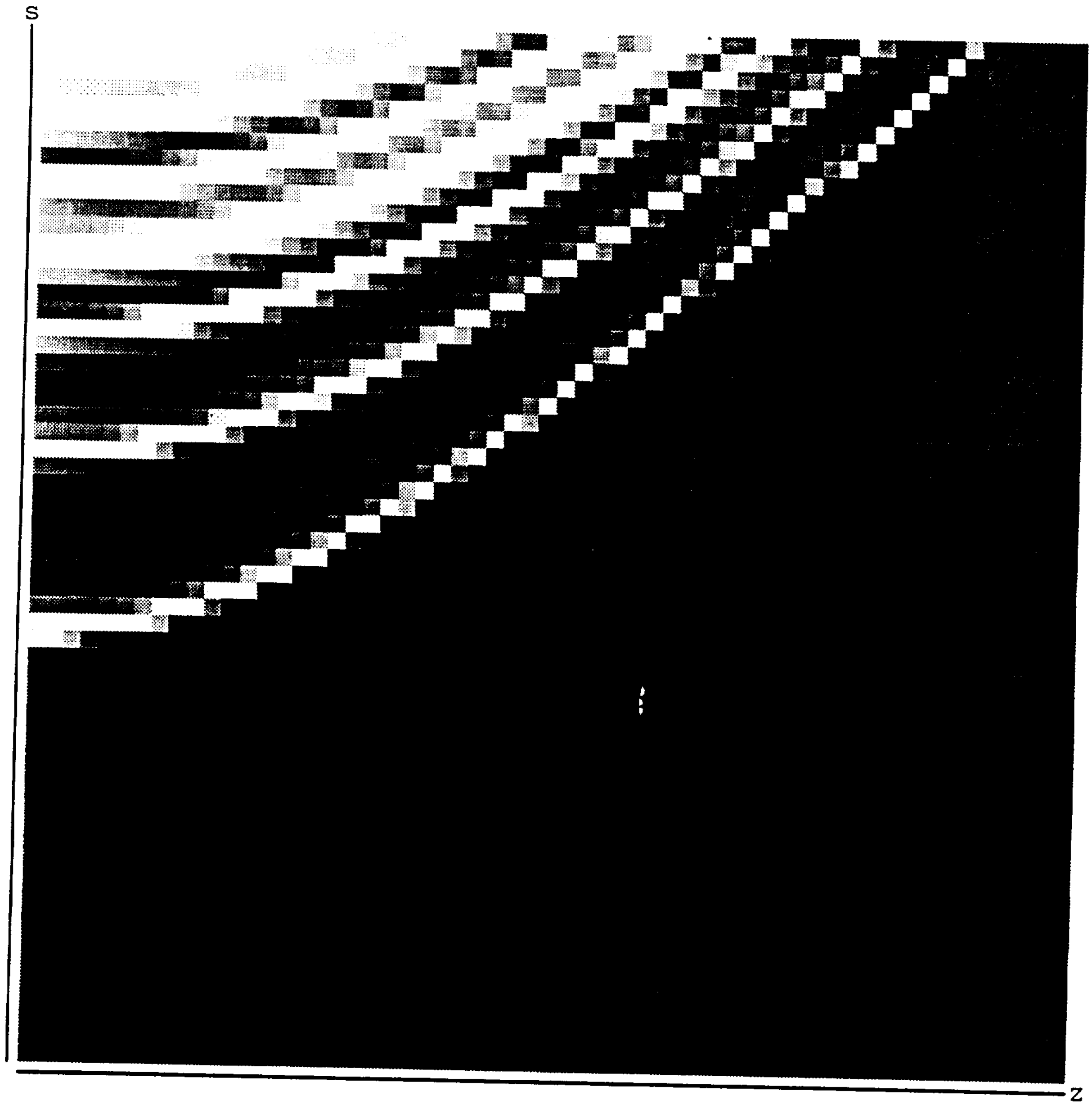

— FIG 2 —

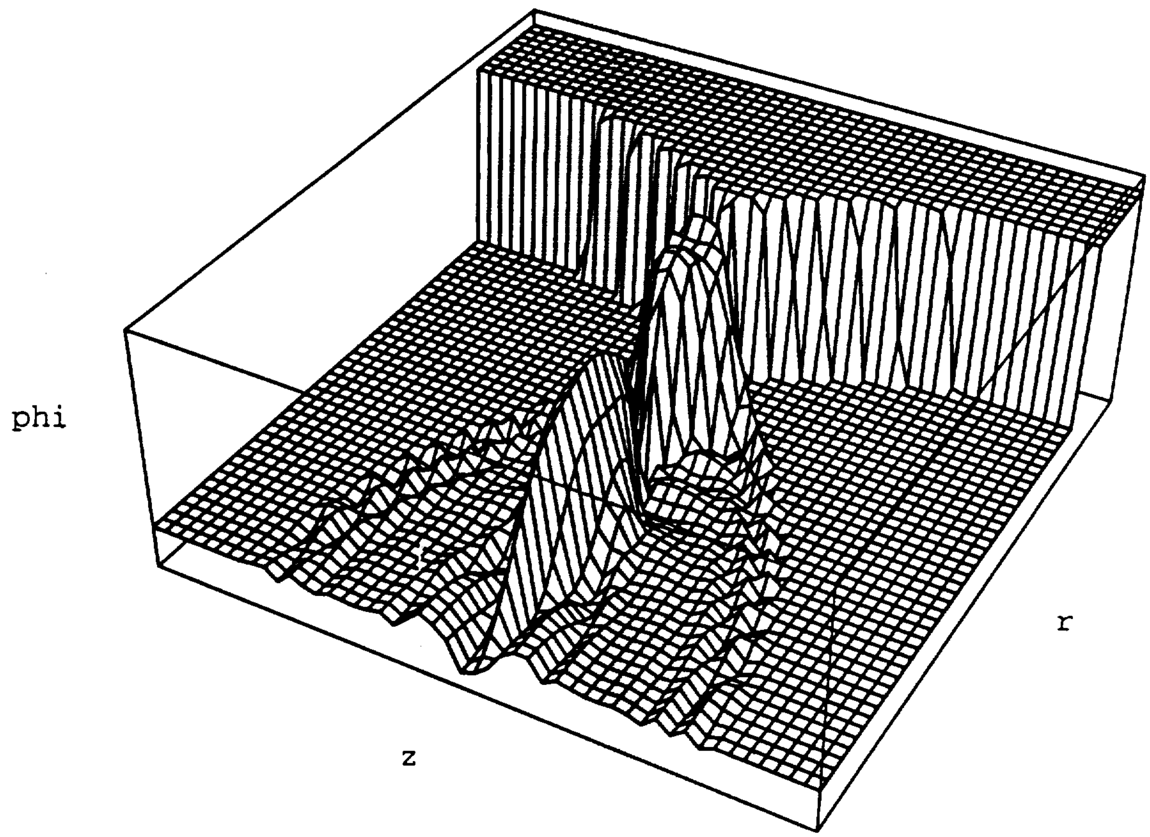

- FIG 3b -

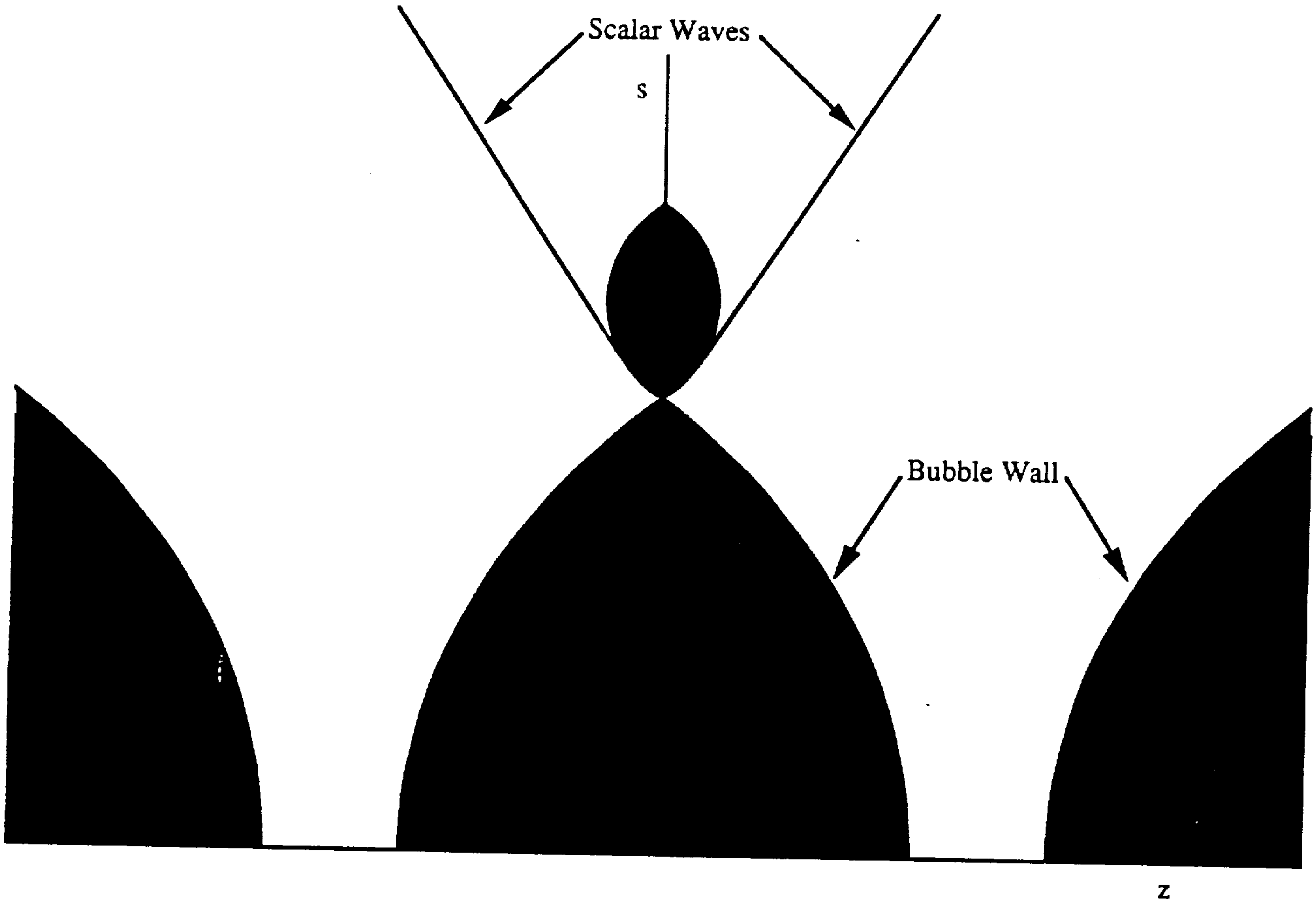

— FIG 4a —